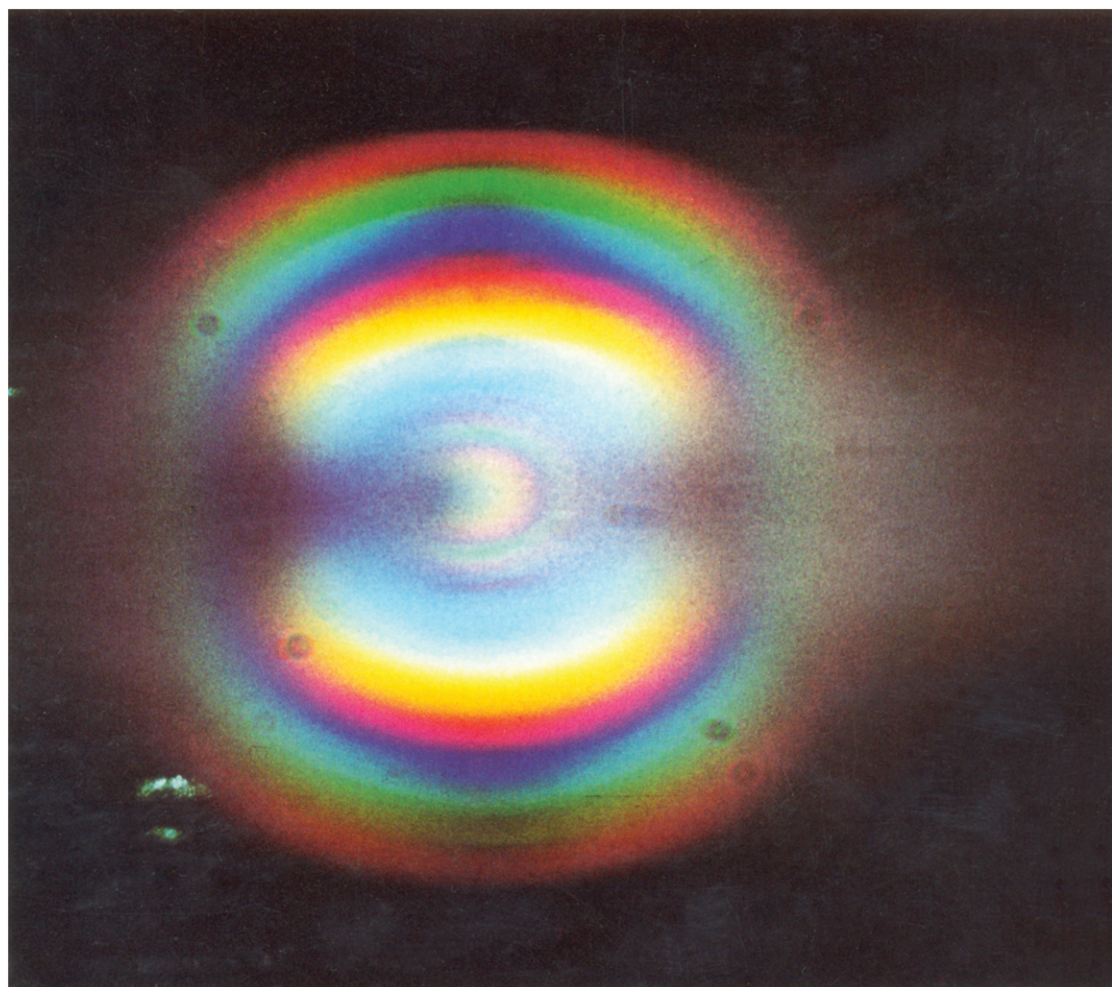


North-Holland

Handbook on

Synchrotron Radiation

| Volume 2 | Edited by **Geoffrey V. Marr** |



| Series Editors: **E.-E. Koch, T. Sasaki** and **H. Winick** |

HANDBOOK ON SYNCHROTRON RADIATION

Series editors

ERNST-ECKHARD KOCH

*Fritz-Haber Institut der Max-Planck-Gesellschaft, Faradayweg 4–6,
1000 Berlin 33/Dahlem*

TAIZO SASAKI

*Department of Material Physics, Faculty of Engineering Science, Osaka University,
Toyonaka-shi, Osaka 560, Japan*

HERMAN WINICK

*Stanford Synchrotron Radiation Laboratory, SLAC, Bin 69, P.O. Box 4349,
Stanford, CA 94305, USA*

HANDBOOK ON SYNCHROTRON RADIATION

VOLUME 2

Edited by

GEOFFREY V. MARR

*Department of Physics, Natural Philosophy Building,
Aberdeen University, Aberdeen AB9 2UE, Scotland*



1987

NORTH-HOLLAND

AMSTERDAM · OXFORD · NEW YORK · TOKYO

© Elsevier Science Publishers B.V., 1987

All rights reserved. No part of this publication may be reproduced, stored in a retrieval system, or transmitted, in any form or by any means, electronic, mechanical, photocopying, recording or otherwise, without the prior permission of the publisher, Elsevier Science Publishers B.V. (North-Holland Physics Publishing Division), P.O. Box 103, 1000 AC Amsterdam, The Netherlands. Special regulations for readers in the USA: This publication has been registered with the Copyright Clearance Center Inc. (CCC), Salem, Massachusetts. Information can be obtained from the CCC about conditions under which photocopies of parts of this publication may be made in the USA. All other copyright questions, including photocopying outside of the USA, should be referred to the publisher. USA, should be referred to the publisher.

ISBN: 0 444 87046 6

Published by:

North-Holland Physics Publishing
a division of
Elsevier Science Publishers B.V.
P.O. Box 103
1000 AC Amsterdam
The Netherlands

Sole distributors for the USA and Canada:
Elsevier Science Publishing Company, Inc.
52 Vanderbilt Avenue
New York, NY 10017
USA

Library of Congress Cataloging in Publication Data

(Revised for Vol. 2)

Handbook on synchrotron radiation

Vol. 2 edited by Geoffrey V. Marr.

Includes bibliographies and indexes.

1. Synchrotron radiation—Handbooks, manuals, etc.

I. Koch, Ernst-Eckhard, 1943– . II. Marr, Geoffrey V.

QC793.5.E627H37 1983 539.7'2112 83-12116

ISBN 0-444-86425-3 (Set)

ISBN 0-444-86709-0 (U.S. : V. 1a)

ISBN 0-444-86710-4 (U.S. : V. 1b)

Printed in The Netherlands

PREFACE

Volume 1 of this series contained an extensive list of topics which attempted to review the characteristics of Synchrotron Radiation, the instrumentation and principles of various research applications for a branch of scientific activity which, following two decades of vigorous research, shows no sign of reducing its rate of development in the foreseeable future. Volume 2 of this series concentrates on the use of synchrotron radiation which covers that region of the electromagnetic spectrum which extends from about 10 eV to 3 keV in photon energy, and is essentially the region where the radiation is strongly absorbed by atmospheric gases, and so has to make extensive use of a high vacuum to transport the radiation to the workstation, and where the presence of hard X-rays can cause extensive damage to both the optics and the targets used in the experimental rigs. In order to keep the volume to a reasonable size, a selection of topics has been chosen and attention has been limited essentially to the disciplines of physics and chemistry.

The first three chapters are concerned with the synchrotron radiation source and its beam lines, with attendant facilities of data collection needed to exploit the VUV to soft X-ray radiation. The following three chapters concentrate on the problems of some free atom and molecule studies, while the final five chapters cover surface and solid state phenomena. It is hoped that this material will be of interest to the research student or newcomer to the techniques of exploiting the radiation from a large multi-user facility, as well as providing material of use to the researcher who wishes to consider new developments or the use of techniques, as yet unexplored, where synchrotron radiation may be significant.

Each of the 21 authors has made a substantial contribution to the volume and I would like to take this opportunity of expressing my appreciation to each and every one of them. I hope that they will feel that the final result represents a suitable vehicle for their reviews and for their comments on the future use of Synchrotron Radiation.

As volume editor I am indebted to the general editors to the series for their help in getting this volume under way. In particular, it is a pleasure to express my appreciation to Ernst Koch, who as editor of Volume 1 and subsequently series editor with Dr. Sasaki and Dr. Winick, did much to support early efforts in the assembly of topics for Volume 2.

It is a fact that this volume would not have been possible without the very capable help received from my secretary Carole Faulkner, who in the preparation

of manuscript and through the efficient handling of the secretarial work involved, ensured that material reached the publishers on time. North-Holland, as ever, have continued to handle this contribution to the Handbook Series in their usual competent way. Their patience and understanding in dealing with this volume editor is much appreciated.

Geoffrey V. Marr
Aberdeen 1987

CONTENTS

<i>Preface</i>	v
<i>Contents</i>	vii
<i>Contributors to Volume 2</i>	xi
1. Synchrotron radiation sources.	1
<i>I.H. Munro and G.V. Marr</i>	
1. Introduction 3	
2. Synchrotron radiation sources in the soft X-ray (SXR) and vacuum ultraviolet (VUV) regions 6	
3. The prospects for increasing the brilliance of SR sources in the soft X-ray region 14	
4. Synchrotron radiation source installations 19	
References 20	
2. Optical engineering	21
<i>J.B. West and H.A. Padmore</i>	
1. Introduction 23	
2. The synchrotron radiation source 24	
3. Mirrors 35	
4. Diffraction grating optics 56	
5. Beam line layout 84	
6. Optical components 99	
7. Beam line auxiliary equipment 109	
8. Conclusion 116	
References 117	
3. Data aquisition and analysis systems	121
<i>P.A. Ridley</i>	
1. Introduction 123	
2. Data aquisition electronics 124	
3. Local computer systems 148	
4. Data processing facilities 157	
References 170	
4. High resolution spectroscopy of atoms and molecules including Faraday rotation effects	175
<i>J.P. Connerade and M.A. Baig</i>	
1. Introduction 177	
2. High resolution spectra of atoms 177	

- 3. High resolution spectra of molecules 212
- 4. SR experiments with polarised radiation 230
- 5. Conclusion 236
- References 237

- 5. Resonances in molecular photoionization 241
J.L. Dehmer, A.C. Parr and S.H. Southworth
 - 1. Introduction 243
 - 2. Shape resonances 245
 - 3. Autoionization 263
 - 4. Triply differential photoelectron measurements – experimental aspects 275
 - 5. Case studies 280
 - 6. Survey of related work 330
 - 7. Prospects for future progress 334
 - Appendix. A bibliography on shape resonances in molecular photoionization through early 1985 336
 - References 342

- 6. Molecular photodissociation and photoionization 355
I. Nenner and J.A. Beswick
 - 1. General introduction 357
 - 2. Experimental methods 361
 - 3. Selected examples 382
 - 4. Miscellaneous and future trends 455
 - References 458

- 7. Surface science with synchrotron radiation 467
I.T. McGovern, D. Norman and R.H. Williams
 - 1. Introduction 469
 - 2. Techniques 469
 - 3. Clean surfaces 476
 - 4. Surfaces with adsorbates 500
 - 5. Interfaces 521
 - 6. Conclusions 533
 - References 533

- 8. Metal–semiconductor interface studies by synchrotron radiation techniques 541
L.J. Brillson
 - 1. Introduction 543
 - 2. Metal–semiconductor interactions and electronic properties 544
 - 3. Soft X-ray photoemission spectroscopy for microscopic interface characterization 547
 - 4. Chemical bonding at metal–semiconductor interfaces 549
 - 5. Metal–semiconductor interdiffusion 576
 - 6. Fermi level pinning and semiconductor band bending 582

7. Other synchrotron radiation techniques for interface analysis	594
8. Conclusions and future directions	600
References	603
9. Inner shell photoelectron process in solids	611
<i>A. Kotani</i>	
1. Introduction	613
2. Fundamental theory of many-body effects in inner shell photoelectron process	614
3. Simple metals	623
4. Rare earth metals and compounds	627
5. Transition metals and compounds	639
6. Related topics	650
7. Concluding remarks	656
Appendix. Derivation of basic photoemission formulae	657
References	660
10. Surface core level shift	663
<i>Y. Jugnet, G. Grenet and Tran Minh Duc</i>	
1. Introduction	665
2. Surface-bulk core level shift for clean surfaces	666
3. Applications	693
4. Conclusion	718
References	719
11. Optical constants	723
<i>D.W. Lynch</i>	
1. Introduction	725
2. Definitions	726
3. Sample characteristics	738
4. Measurement methods	742
5. Summary	762
6. Some examples	764
7. Comments on data collections and recent literature	770
Appendix. Recent literature reference to optical data for $E \geq 6 \text{ eV}$	772
References	775
<i>Author index</i>	785
<i>Subject index</i>	829

This page intentionally left blank

CONTRIBUTORS TO VOLUME 2

- M.A. Baig, *Physikalisches Institut, Universität Bonn, Nussallee 12, Bonn, Fed. Rep. Germany**.
- J.A. Beswick, *LURE, Centre National de la Recherche Scientifique et Université de Paris Sud, 91405 Orsay, France.*
- L.J. Brillson, *Xerox Webster Research Center, 800 Phillips Road W114, Webster, NY 14580, USA.*
- J.P. Connerade, *The Blackett Laboratory, Imperial College, London SW7 2AZ, UK.*
- J.L. Dehmer, *Argonne National Laboratory, Argonne, IL 60439, USA.*
- G. Grenet, *Institut des Sciences de la Matière and Institut de Physique Nucléaire de Lyon (and I N2 P3), Université Claude Bernard Lyon-1, 43 Bd. du 11 Novembre 1918, F69622 Villeurbanne Cédex, France.*
- Y. Jugnet, *Institut des Sciences de la Matière and Institut de Physique Nucléaire de Lyon (and I N2 P3), Université Claude Bernard Lyon-1, 43 Bd. du 11 Novembre 1918, F69622 Villeurbanne Cédex, France,*
- A. Kotani, *Department of Physics, Faculty of Science, Tohoku University, Sendai 980, Japan*
- D.W. Lynch, *Department of Physics and Ames Laboratory-USDOE, Iowa State University, Ames, IA 50011, USA*
- G.V. Marr, *Department of Physics, Natural Philosophy Building, Aberdeen University, Aberdeen AB9 2UE, Scotland.*
- I.T. McGovern, *Department of Pure and Applied Physics, Trinity College, Dublin, Republic of Ireland.*
- I.H. Munro, *Science and Engineering Research Council, Daresbury Laboratory, Daresbury, Warrington WA4 4AD, UK.*
- I. Nenner, *Commisariat à l'Energie Atomique, IRDI, Department de Physico-Chimie, Centre d'Etudes Nucléaires de Saclay, 91191 Gif sur Yvette, France and LURE, Centre National de la Recherche Scientifique et Université de Paris Sud, 91405 Orsay, France.*
- D. Norman, *Science and Engineering Research Council, Daresbury Laboratory, Warrington, WA4 4AD, UK.*
- H.A. Padmore, *Science and Engineering Research Council, Daresbury Laboratory, Daresbury, Warrington WA4 4AD, UK.*
- A.C. Parr, *Synchrotron Ultraviolet Radiation Facility, National Bureau of Standards, Gaithersburg, MD 20899, USA.*

* Present address: Physics Department, Quaid-i-Azam University, Islamabad, Pakistan.

- P.A. Ridley, *Science and Engineering Research Council, Daresbury Laboratory, Daresbury, Warrington WA4 4AD, UK.*
- S.H. Southworth, *Los Alamos National Laboratory, Los Alamos, NM 87545, USA.*
- Tran Minh Duc, *Institut des Sciences de la Matière and Institut de Physique Nucléaire de Lyon (and I N2 P3), Université Claude Bernard Lyon-1, 43 Bd. du 11 Novembre 1918, F69622 Villeurbanne Cédex, France.*
- J.B. West, *Science and Engineering Research Council, Daresbury Laboratory, Daresbury, Warrington WA4 4AD, UK.*
- R.H. Williams, *Physics Department, University College, Cardiff, UK.*

CHAPTER 1

SYNCHROTRON RADIATION SOURCES

I.H. MUNRO

*Science and Engineering Research Council, Daresbury Laboratory,
Daresbury, Warrington WA4 4AD, England*

G.V. MARR

*Department of Physics, Natural Philosophy Building, Aberdeen University,
Aberdeen AB9 2UE, Scotland*

Contents

1. Introduction	3
2. Synchrotron radiation sources in the soft X-ray (SXR) and vacuum ultraviolet (VUV) regions	6
2.1. The properties of storage ring sources	6
2.2. Collimation of synchrotron radiation and its polarisation	8
2.3. The radiated spectrum	9
2.4. The photon source in practice	10
2.5. The time modulation of the source	14
3. The prospects for increasing the brilliance of SR sources in the soft X-ray region	14
3.1. Insertion devices	15
3.2. Undulator radiation	17
3.3. Coherence	18
4. Synchrotron radiation source installations.	19
References	20

This page intentionally left blank

1. Introduction

The synchrotron is a machine which is used by physicists to produce high energy (GeV) charged particles. This type of accelerator confines the particles (usually electrons) by magnetic fields so as to cause them to move over approximately circular orbits. It then accelerates them to speeds approaching that of light before they are extracted for collision experiments. The centripetal force acting on the relativistic electrons causes them to radiate electromagnetic radiation predominantly in the vacuum ultraviolet and soft X-ray regions. The radiation is emitted in a narrow cone in the direction of the fast moving electrons so that for a closed circular orbit the radiation appears as a narrow fan emitted tangential to the electron orbit and centred about the orbit plane.

Many individuals have been involved in the development of the classical electrodynamical theory of synchrotron radiation. It effectively began with the early work of Lienard (1898), was developed by Schott (1912) in an attempt to solve the radiation problem of the hydrogen atom and is now to be found in standard texts (Jackson 1975) as well as being the subject of detailed reviews (see Handbook on Synchrotron Radiation, Vol. 1: Koch et al. 1983, Krinsky et al. 1983). It is not the purpose of the present chapter to repeat these reviews, but to attempt a brief summary of the features of modern synchrotron radiation sources so that intended users of these facilities may be aware of their properties and so that it may serve as an introduction to the following chapters in the present volume where the exploitation and use of the vacuum ultraviolet to soft X-ray radiation is discussed.

The past 30 years have seen synchrotron radiation sources and their user communities “come of age”. During the 1960’s and 1970’s, each novel experimental result had a good chance of leading to the generation of a whole new area of experimental science. The literature contains several important examples including the development of mirror and grating systems for the vacuum region, cross section related studies of atoms and molecules, topography, bulk and surface EXAFS, small angle diffraction, soft X-ray imaging and many others. The significance of these advances was often enhanced at the time because of their interdisciplinary nature, drawing together the rather different skills of the physicist, chemist and bioscientist in the solution of problems of mutual interest.

A somewhat different but rather more obvious transition has occurred in the properties of the sources themselves. Almost all synchrotron radiation research until well into the 1970’s was conducted using electron accelerators (synchrotrons) whose primary objective was to carry out research into the properties of elementary particles. This “parasitic” exploitation of the unwanted electromagnetic radiation produced by the unavoidable energy loss from circular accelerators, gradually devolved into a relationship between the exploiters of synchrotron radiation and the high-energy physicists, which is now called “symbiotic”. As a

consequence, the past decade has seen the appearance of a community of accelerator physicists who have been actively encouraged to design machines to maximise the output of synchrotron radiation from accelerators whose emittance is designed to be as small as is physically compatible with a source which is expected to run for more than 5000 hours per year. The costs of such a machine, together with the very high level of demand for access from a large number of scientific groups, decrees that predictable and reliable operation of the source is the paramount requirement of the designers. In addition, many of the user scientists originally had little or no understanding of the source, nor of working at a large institutionalized facility. With 24 hour usage required, shift working of technical staff simply to maintain a functioning source is necessary and to maintain the experimental workstations in good working order a scientific support staff must be always on call. Support staff are also needed to develop new workstations and to provide the software essential for equipment control, data collection and analysis. The synchrotron radiation facility is a large, expensive, and complex organisation, devoted to the provision of electromagnetic radiation to a wide range of experimental rigs, and service a community with diverse scientific backgrounds. Differing methods for tackling these problems have been established at the various facilities around the world, and discussions of cost effective exploitation is increasingly prominent in the planning and *modus operandi* at each synchrotron radiation facility.

The first generation of purpose built sources of synchrotron radiation were designed through the 1970's as electron storage rings with the synchrotron radiation coming from the use of dipole magnets to bend the stored electron beam into a closed loop. There has been a steady increase in the stable circulating beam current which can be sustained by a storage ring for long stored beam periods. Present day accelerators are normally expected to support circulating currents of at least 100 mA (often <500 mA is achieved) for periods of several hours. This represents probably a tenfold increase in "ampere hours" in as many years. Less dramatic has been the improvement in control of the electron beam position and direction at the photon beam source points. The essential requirement for all photon beam lines from such storage rings is for direction sensors to interactively define the operating parameters of the storage ring. Source control simultaneously at many positions around each storage ring is difficult due to the interdependence of electron beam dynamics on conditions prevailing at different magnets round the ring. Nevertheless, beam stability for the majority of present day users is an essential requirement.

At a very early stage in the development of synchrotron radiation sources it was realised that the ability to harness radiation from a linear array of dipole magnets could provide a means of maximising the photon flux at a workstation and would be more feasible than attempting to store extremely high circulating ring currents (see Kincaid 1977). The transformation of the design criteria associated with the European Synchrotron Radiation Facility (the ESRF) illustrates rather dramatically this evolution in source design which has taken place between approximately 1977 and 1987. The original ESRF design was for a storage ring of fairly high

current and small electron beam cross section with synchrotron radiation being derived principally from dipole magnets and wigglers (wavelength shifters). The present (Buras and Tazzari 1985) design however is based exclusively on "insertion devices" where dipole magnets are used essentially only to transfer the circulating beam from one undulator or wiggler device to the next.

The specificity of undulator radiation (in terms of spectral output, beam emittance and polarisation) has led to the present day philosophy in which the source parameters are tailored as fully as possible to match the specific needs of a particular experiment. There is the immediate example of synchrotron radiation used in lithography where the storage ring is exclusively designed, constructed and operated in a manner dedicated to a single set of technical requirements.

The evolution of synchrotron radiation sources as sources of hard and soft X-rays is summarised in fig. 1. It incorporates conventional X-ray sources which can operate only with very poor efficiency. The total radiated (photon) power is typically only 0.1% of the input power in such devices which, because of Joule heating, are unable to exploit input power levels of greater than approximately 100 kW. All sources of this kind radiate approximately isotropically and the unpolarised radiated spectrum contains spectral lines superimposed on a back-

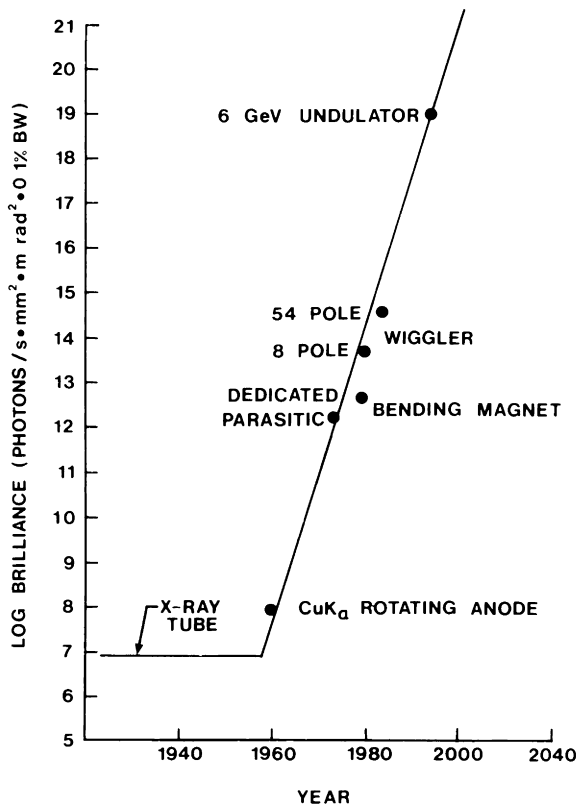


Fig. 1. History of X-ray sources.

ground continuum. The source size also is limited by thermal load considerations to a value approximately a few 10^{-8} to 10^{-5} m². The source brilliance is therefore fundamentally limited to less than 10^9 .

The first generation of synchrotron radiation sources (that is storage ring designs approximately up to the present time) have a high efficiency for conversion of input power into radiated power in a broadband (white) spectrum. The maximum input power is restricted mainly by the cost of producing and coupling a high level RF source (the klystron) to a storage ring. The total input power to present day rings is usually greater than 100 kW and up to 1 MW and beyond will be perfectly feasible in high energy storage rings. The source size (the electron beam cross section) remains comparable with the best conventional X-ray microfocuss source in the region from approximately 10^{-8} m² to 10^{-6} m². However, the beam divergence and degree of polarisation (usually approximately 95%) which are dictated by the relativistic properties of the source, push up the source brilliance by at least 10^4 times above that of non-synchrotron-radiation sources.

The evolutionary leap *in brilliance* associated with undulator sources is not based on greater source input power (which remains approximately <2 MW) nor on increased circulating current, but on the reduction in source emittance and the increase in undulator source coherence. By the mid-1990's, linear or circularly polarised radiation should be produced from undulators containing from 100 to 1000 periods. The source size of 10^{-8} m², source divergence of $\sim 10^{-5}$ radians and intrinsic spectral purity from 1% to 0.1% will yield an unprecedentedly high brilliance approaching 10^{19} photons per s mm² mrad² 0.1% bandwidth. This projection must surely tremendously expand the boundaries in science and for example could lead on to the study of exceedingly small samples measured in short time periods. Very high momentum resolution in scattering and high energy resolution in spectroscopic experiments, together with the potential for high spatial resolution overall for imaging studies are other features of future undulator radiation which will be exploited in future.

2. Synchrotron radiation sources in the soft X-ray (SXR) and vacuum ultraviolet (VUV) region

2.1. The properties of storage ring sources

The optical cross section and effective length of a Synchrotron Radiation Source (SRS), together with its spectral characteristics, angular divergence and time structure are each defined by the parameters of the ring, which will have been selected in each case to optimise the match between user experimental needs, minimum source construction and operation costs. Although a full discussion of the physics of storage ring sources and the technological problems in their construction is reviewed elsewhere (see for example Krinsky et al. 1983 and Sands 1970) it is important to summarise the relationships between the storage ring parameters and the properties of the emitted radiation.

Radiation will be emitted when any charged particle is accelerated. The case of synchrotron radiation is restricted (normally) to electrons or positrons confined in a circular accelerator where they go around the ring at a fixed frequency (ν) given by

$$\nu = \frac{v}{2\pi R}, \quad (1)$$

where R is the radius of the electron orbit and v is the particle speed.

In practice, v will be very close to the speed of light, c . Looking back along a soft X-ray beam line into any synchrotron radiation source, a laboratory-based observer will “see” the electron or positron emitting radiation from a frame of reference moving towards him with velocity v relative to his own (hopefully stationary) reference frame. Transposing from the reference frame of the source to that of the observer results in dramatic changes in the form of the emitted radiation pattern and predicts many unusual results all of which have been shown to be in agreement with observation.

The properties of a charged particle in the ring will be governed by its instantaneous momentum, which is equal to the product of the magnetic field strength B (in tesla) the orbit radius R (in metres) and the particle charge.

In fact the radius of curvature of the particle orbit is given by

$$R = 3.3 E/B, \quad (2)$$

where E is the electron energy in GeV. Using iron electromagnets, where B_{\max} is typically 1.2 T, the bending radius will be 5.6 m for example for a 2 GeV storage ring. For higher energy rings (producing “harder” X-rays) this radius will be increased. Of course the average radius of a storage ring is always greater than the particle bending radius because of the extra lengths of orbit (straight sections) used to connect dipole magnets.

A typical mean radius for a 2 GeV machine (the Daresbury SRS) is 15 m. When a specially constructed high field bending magnet is used (such as the 5 T superconducting wiggler at the Daresbury Laboratory SRS) then the electron orbit radius will be correspondingly reduced – in this case to ~ 1.3 m in the vicinity of the wiggler.

The energy lost by each electron in a storage ring per single revolution is given by

$$\Delta E = \frac{88.5 E^4}{R} \text{ keV}, \quad (3)$$

which corresponds to about 250 keV for the SRS, or several photons per electron per revolution, where the energy of each photon ($h\nu$) is given by $h\nu$ (eV) = $12.4/\lambda$ (Å). If a corresponding amount of energy were not to be fed into the storage ring via the RF system then the electrons would rapidly lose energy and spiral inwards to collide with the vacuum vessel or a target “scraper”.

The total power, P , radiated by a storage ring is given by the total number of electrons contained in the ring (measured by the mean circulating current I in amperes) and is given by

$$P = 88.5 E^4 I / R \text{ (kW)}. \quad (4)$$

The total power radiated by each relativistic electron is in fact

$$P = \frac{2}{3} \frac{e^2 c}{R^2} \left(\frac{E}{m_0 c^2} \right)^4 \left(\frac{1}{4\pi\epsilon_0} \right) \text{ (W)}, \quad (5)$$

where m_0 is the rest mass of the charged particle. This expression reveals why it is that protons radiate far less power than electrons when accelerated to the same energy E . While electrons and positrons are equally effective as synchrotron radiation sources, a proton at the same energy will radiate only 10^{-13} as much power. Alternatively, to extract as much synchrotron radiation from a proton as from an electron storage ring would require 1836 times the energy!

For the Daresbury SRS, operating at above 100 mA circulating current (that is with approximately 10^{12} electrons in the ring), at least 50 kW of radiated power will be produced, necessitating the use of a 500 MHz klystron with an output power of at least 100 kW.

The instantaneous synchrotron radiation beam divergence is set by the electron energy (i.e., the source velocity) and is given roughly by the angle $1/\gamma$ where $\gamma = (1 - v^2/c^2)^{-1/2}$. For a medium (2 GeV) energy storage ring such as the SRS this will correspond to a cone angle of somewhat less than one milliradian (where 1 mrad \sim 200 seconds of arc).

It is important to establish the radiative power loading on a target which results from the highly directional nature of synchrotron radiation. The power emitted in the horizontal plane may be shown to be

$$P_{\text{Hor}} = 4 \times 10^{-3} E^3 B I \text{ (W/rad)}. \quad (6)$$

For the SRS operating at 2 GeV and approximately 250 mA this yields approximately 10 W/mrad from a dipole magnet. For the X-ray region, the vertical collimation of the beam is also \sim 1 mrad and the power will fall on an area of \sim 10 mm² at 10 m from the source. In many experiments, the bulk of this power will fall on a mirror, crystal or grating which obviously must be radiation resistant. For multipole wiggler devices and undulators, the power loading on the first element can be enormous (up to approximately 100 W/mm²) and radiation and thermal damage or distortion effects on the instrumentation or on the sample may ultimately limit the benefits from sources planned to have exceptionally high brilliance.

2.2. Collimation of synchrotron radiation and its polarisation

The detailed calculation of radiated power from a storage ring allows the intensity emitted to be expressed in terms of the radiation polarised with either the E

vector perpendicular or parallel to the electron orbit plane. Viewed in the plane of the orbit, the radiation is 100% plane polarised with the E vector in the plane of the orbit. Out of this plane both components of polarisation are seen and the degree of polarisation is wavelength-dependent. Nevertheless, the degree of polarisation is at least 75% for radiation integrated over all wavelengths and all vertical angles. Radiation from an electron storage ring is therefore either plane polarised or elliptically polarised, depending on the beam line conditions and the wavelength region of the spectrum.

The collimation of emitted radiation can be related to λ_c , the so-called “critical wavelength” which divides into two equal parts the total radiated power (i.e., half at wavelengths greater than λ_c and half at wavelengths less than λ_c). For a given λ_c , the radiation divergence angle decreases as wavelength is reduced. However, for a particular wavelength, the divergence angle reduces as λ_c is increased and, since λ_c varies inversely as the electron energy, lower energy accelerators produce less divergent radiation than high energy accelerators.

The intensity distribution in the vertical direction can be satisfactorily described by a Gaussian over a wide wavelength range. The actual vertical opening angle is less than $1/\gamma$ below λ_c , roughly equal to $1/\gamma$ at λ_c and increases to several times $1/\gamma$ for $\lambda \sim 100 \lambda_c$.

2.3. The radiated spectrum

The unique “white” continuum associated with all synchrotron radiation sources results from the extremely high electron velocity with respect to the laboratory experimental station. The observer will gather radiation only from a small opening angle ($\sim 1/\gamma$) which corresponds to a length of orbit about R/γ . The radiation pulse produced for a time Δt will appear to the laboratory-based user to be relativistically reduced, corresponding to $R/c\gamma^3$. A frequency analysis of such a short duration pulse reveals harmonics of the orbit frequency (usually ~ 1 MHz) up to $1/\Delta t$, i.e., the pulse analysis reveals angular frequencies up to γ^3 times the orbit frequency. In practice, the individual harmonics cannot be resolved at such high frequencies and so the radiation appears to have a continuous spectrum extending from the microwave region to very short wavelengths about $2\pi R/\gamma^3$. In practice, the overall spectral profile rather resembles that of a black-body radiator at an extremely high temperature: 10^7 K or so.

The detailed spectral profile calculations incorporate the critical wavelength, λ_c (Å), which is defined to be the wavelength which divides the power spectrum into two equal parts:

$$\lambda_c = 19(BE^2)^{-1} . \quad (7)$$

The radiated power as a function of wavelength in a 0.1% bandwidth (where $\Delta\lambda = 10^{-3} \lambda$) per milliradian of horizontal angle is given by

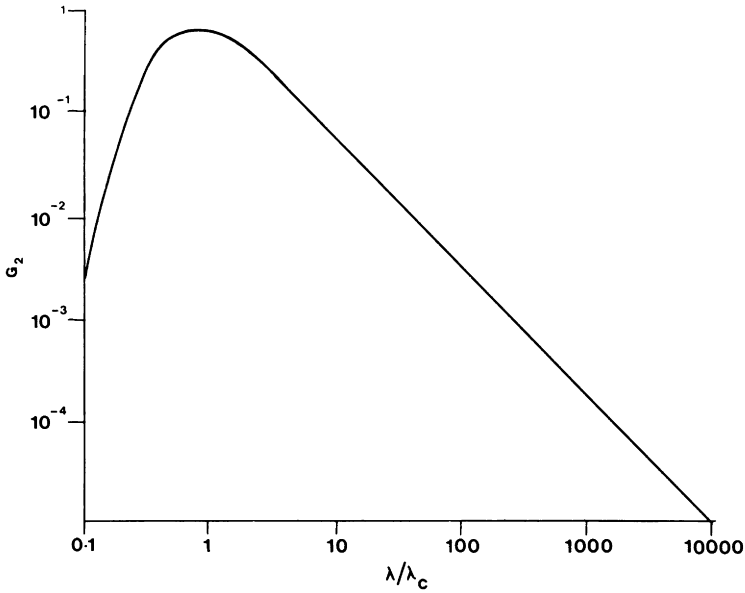


Fig. 2. Radiated power as a function of wavelength in a 0.1% bandwidth per milliradian of horizontal angle.

$$P(\lambda) = 8.7 \times 10^{-3} \frac{E^4}{R} G_2 \frac{\lambda}{\lambda_c} I, \quad (8)$$

where $G_2(\lambda/\lambda_c)$ is a Universal function (Krisinsky et al. 1983) and is shown in fig. 2. The peak power is radiated at $\lambda = 0.7 \lambda_c$. Almost all the radiated power is contained within the range $0.2 \lambda_c < \lambda < 10 \lambda_c$.

For users of synchrotron radiation, the radiated spectrum is almost always presented as a photon flux, $N(\lambda)$, rather than power. Figure 3 shows the Universal distribution of photon flux in synchrotron radiation given by

$$N(\lambda) = 2.5 \times 10^{14} E G_1 \frac{\lambda}{\lambda_c} I. \quad (9)$$

Useful flux is normally assumed to extend from $\lambda > 0.1 \lambda_c$ with the maximum occurring at $\lambda = 4 \lambda_c$. The flux then falls off extremely slowly to longer wavelengths. For the Daresbury SRS, with $\lambda_c = 3.9 \text{ \AA}$, the maximum photon flux at 2 GeV and 300 mA is $\sim 3 \times 10^{13} \text{ photons s}^{-1} \text{ mrad}^{-2}$ in 0.1% bandpass and is typical for a dipole magnet source at this current.

2.4. The photon source in practice

The properties of an actual radiation source, viewed from the laboratory reference frame, are determined partly by the synchrotron radiation characteristics

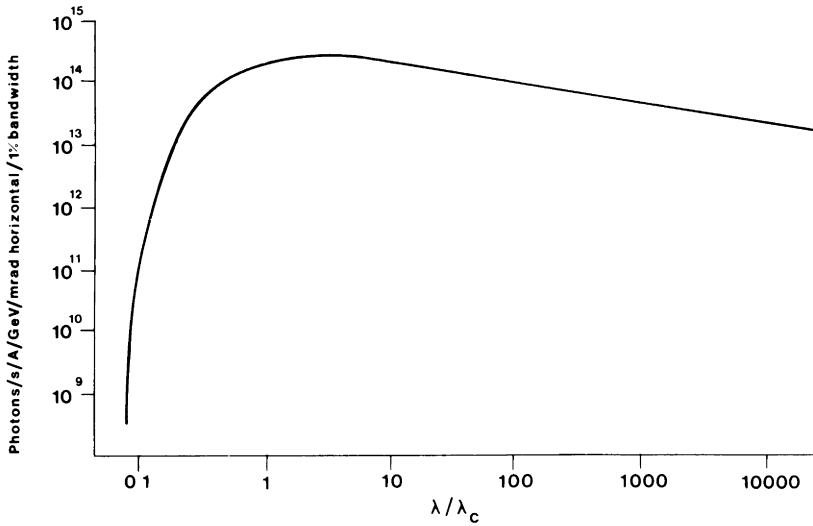


Fig. 3. Universal distribution of photon flux in synchrotron radiation.

associated with a single electron at the energy of the accelerator and partly by the statistical spread in position, direction and time of the large number of electrons ($\sim 10^{12}$ or so for $I > 100$ mA) which constitute the circulating beam.

A fundamental constant for any storage ring is its emittance which is conserved at positions around the orbit and is equal to the product of the overall electron beam dimension and divergence in the horizontal (radial) and vertical directions. In principle, the vertical and horizontal emittances are independent although in practice the source properties can be modified by altering the degree of coupling between the two components. The emittances are determined by complex functions which describe the damping and focussing processes in the electron beam around the ring. A good indication of the range of storage ring emittance values is given in table 1. For example, the emittance at the Daresbury SRS results in a full width at half maximum intensity source size of approximately 1 mm^2 . Obviously, this value will define the size of the image at a sample or will limit the minimum slit size to be used in a monochromator. Similarly, the electron beam divergence will contribute to the intrinsic divergence of the synchrotron radiation from a source. In present day storage rings, however, the small values for electron beam emittance yield electron beam divergence values which are < 1 mrad and are therefore significant only at the very shortest wavelengths.

For the future, it will be important for the vertical and horizontal source sizes to be as small as possible ($< 100 \mu\text{m}$) in order to allow good source size limited resolution to be achieved with entrance slitless monochromators and to permit monochromators to be developed to exploit both polarisation components of radiation to be used from the storage ring. Obviously, the exploitation of such very small source sizes also imposes the requirement that the beam position can be reproducibly controlled to within the dimensions of the beam and that no oscillations or long term drifts in position should be permitted.

Table 1
Summary of synchrotron radiation sources (worldwide). (D – dipole magnet, W – wiggler, U – undulator, and FEL – free electron laser.)

	λ_c (Å)	Approx. no. expt. stations	Emittance ($10^{-8} \pi$ mrad)	Insertion devices	Operating energy (GeV)	Operating current (mA)	Annual hours operation (h)
<i>Brazil</i>							
Campinas – LNRS					2	100	
<i>China</i>							
Beijing – BEPC	2.6	4 (X-ray only)	66	–	2.8	150	Part dedicated, under construction: 1st beam end 1987
Hefei – HESYRL	20	–	9	Undulator planned	0.8	–	Dedicated
<i>European SR Facility</i>							
Grenoble – ESRF	1 (D), 0.86 (U), 0.1 (W)	Approx. 30 by year 2000	0.7	28–30 W or U, as required	6	100–200	Design phase
<i>France</i>							
LURE, Orsay – ACO	39	13	15	1 FEL	0.54	150	1700
– DCI	4 (D), 1.1 (W)	14–20	150	1 W	1.75	200	1300
– SUPERACO	18.5 (D)	19	3	1 W, 1 FEL, 4U	0.8	500 (goal)	Operation commenced 1987
<i>India</i>							
Indore – Ring 1 (approved, under construction)		Design studies in progress . . .			0.45	100	–
– Ring 2 (planned)		Design studies in progress . . .			0.8	–	
<i>Italy</i>							
Frascati – ADONE (part dedicated)	8.3 (D), 4.4 (W)	7	22.5	2 W	1.5	100	1500
Trieste – CARS/AFRODITE (approved)	6.6 (D), 600–6 (U)	10–20	~1	10 U (max.)	1.5	100	Design phase
<i>Japan*</i>							
Tokyo – INSOR	112	6	30	–	0.38	250	1820
Tsukuba (KEK) – Photon Factory	3.1 (D), 0.6 (W)	33	50	1 W, 1 U	2.5	150	2000
– Accumulator Ring	~1 (D)	4	~50	3 (planned)	6	~20	–
– 1.5 GeV ring	250–40	10–20	small	10–13	1.5	150	Planned
Tsukuba (ETL) – TERAS	~10	~10	–	–	0.6	~100	–
Okazaki – UVSOR	29 (D), 8.3 (W)	12	12	1 W, 1 U	0.75	100	–
Konsai – 6–8 GeV ring	~1 (D)	many	small	–	6–8	~100	Proposed
– ~2.5 GeV ring		Low emittance ring for soft X-ray studies					

<i>Sweden</i>								
Lund – MAX	~40	2–6	3	–	0.55	–	–	Operation commenced 1987
<i>Taiwan</i>								
Hsinchu – TLS		Design studies in progress . . .			1.5	200		Partially approved, dedicated
<i>United Kingdom</i>								
Daresbury – SRS	3.9 (D), 0.93 (W), 10–100 (U)	28	11	1 W, 1 U	2.0	300		6000
<i>USA</i>								
Brookhaven – NLSL I	25 (D)	25–30	~14	–	0.75	600		–
– NLSL II	2.5 (D)	30–40	8	1 W, 1 U	2.5	~100		–
Stanford – SPEAR	2.6 (D), 1.2 (8-PW) 1.7 (54-pole)	20–25	45	5	3	80–100		2500
– PEP	–	10–20	15	1 U	14.5	–		–
– SXRL (FEL ring)	–	4	1	1 FEL, 4 for SR	1.0	–		–
Wisconsin – TANTALUS	256	11	23	–	0.24	100		2000
– ALADDIN	12	5–17	11	–	1	~100		2000 (max.)
Ithaca – CESR (CHESS facility)	2.1 to 0.35	6	20	1 W	5.5	40		–
Gaithersberg (NBS) – SURF II	>150	11	27	–	0.28	50 (130 max.)		–
Berkeley – ALS	6.6 (D), ~6–1000 (U)	30–50	1	10 U	>1.5	>100		Design phase
Argonne – 6 GeV ANLS	1 (D), >0.62 (U), >0.1 (W)	30–50	0.8	30 (max.)	6	200		Design phase
<i>USSR</i>								
Novosibirsk – VEPP-2M	–	8	–	2	0.7	–		–
– VEPP-3	–	9	–	2	2.2	–		–
<i>Fed. Rep. Germany</i>								
Hamburg – HASYLAB	1.34 (D), 2.3 (W)	32	27	2 W	3.7	150		1950
– DORIS								
Berlin – BESSY I	19 (D), 28 (U)	31	4	1 U	0.8	600		2700
– BESSY II	5.5 (D), 600–6 (U)	8–16	2	8 U max.	1.5	100		Under construction
– COSY	~15	10–20	250	–	0.56	–		Operational
Bonn – Two synchrotrons	–	–	–	–	0.5, 2.5	–		–

*Other synchrotron radiation source projects are under consideration (or in some cases under construction) at Sendai, Yamagata, Tsukuba (SORTEC), Atsugi (at least 2 rings for N.T.T.) and Hiroshima.

Finally, a storage ring source will appear to an observer to have a very significant depth, L , from which photons are collected and which is simply related to the horizontal aperture, θ , defined to be $L \sim \theta R$. The length of the source apparently will be further extended by virtue of the finite area (horizontal size) of the electron beam with a further contribution arising from the opening angle of the radiation. For a typical source such as the Daresbury SRS, the source length for approximately 5 mrad aperture at the experiment can be as much as 50 mm, necessitating careful representation of the source volume in the ray tracing package used to define the radiation volume in the image plane.

2.5. The time modulation of the source

The electron beam in a storage ring is intrinsically modulated in a longitudinal direction because of the alternating RF field which is used to accelerate the beam. A wide range of accelerating frequencies are used extending from about 1 MHz to 500 MHz. Electrons will be accelerated only if they are in phase with the accelerating field applied when they traverse the RF cavity in the ring. Electrons which are out of phase with the field will receive either too much or too little energy, resulting in an electron orbit which cannot be contained within the vacuum chamber – they collide with the chamber walls and are lost. In phase (or synchronous) electrons are typically confined within a time window which is roughly 10% of the period of the RF and orbit the ring in a series of well defined and regularly spaced bunches.

For accelerators with 500 MHz accelerating fields the bunches are therefore spaced in time by the period of the field ($=2$ ns) and are roughly of 200 ps duration (corresponding to a bunch length of ~ 6 cm f.w.h.m.). In practice, the length of the bunch may be determined by the complex impedance of the orbit chamber in which the electron beam, modulated at high frequency, is contained. The bunch length also tends to increase as the circulating current is increased and short bunch operation is usually limited therefore to currents of about 10 mA or so. The number of electron bunches in a storage ring will have a maximum value given by the ratio of the ring orbit period divided by the RF period. For the SRS this value is 160 bunches. It is possible also to operate many storage rings with electrons effectively confined solely to a single bunch which will then provide all the characteristic properties of synchrotron radiation in terms of its spectral profile, polarisation, etc., but, in the case of the SRS, in ~ 200 ps wide pulses and with a duty cycle of 1/1600!

3. The prospects for increasing the brilliance of SR sources in the soft X-ray region

The properties of synchrotron radiation sources are usually discussed in connection with radiation produced at magnet dipoles and determined at different points around the ring.

The spectral brilliance (defined to be the number of photons per second, per 100 mA circulating current, per mm^2 electron beam source cross section, per mrad^2 , per $0.1\% \Delta\lambda/\lambda$) is expected to have a maximum value of $\sim 10^{13}$ for realistic values of present circulating current and storage ring emittance. The next major step in the quest for high source brilliance will be to increase the number of source points (i.e., magnets), to further reduce the electron beam emittance and the photon beam divergence. Note that the spectral brilliance is normally considered in terms of a cw source. However, when a storage ring is operating in the single bunch mode, the peak (instantaneous) brilliance may be already up to 10^3 times higher than for cw operation.

3.1. Insertion devices

There are three basic types of insertion devices, each of which has some advantage over a normal dipole bending magnet in terms of spectral range, greater flux or brilliance. Insertion devices are appealing to accelerator physicists since they can be incorporated and operated in a storage ring in a largely independent manner. This should offer much more flexibility in terms of the number and types of insertion devices which can be used without serious interaction with the basic beam properties, such as the emittance of the electron beam.

The first device (attempted as early as about 1970 in Wisconsin) was called a wavelength shifter. This is normally a three-pole arrangement based on a central dipole usually operating at a very high field strength. The effect is to reduce the value of λ_c for a particular machine energy and is used at the SRS at Daresbury to provide high flux at $\sim 1.5 \text{ \AA}$ for X-ray diffraction and scattering experiments.

The second type of insertion device, called a multipole wiggler, yields an increase in output flux simply by using a magnetic field which changes periodically in polarity along the length of the device. The multipole wiggler will then act in effect as a series of N independent dipole sources. Unlike a dipole magnet source, however, both the wiggler and multipole wiggler produce a modification of the electron source for a given storage ring current and energy in which the divergence of the synchrotron radiation in the orbit plane is restricted to some extent, according to the deflection of the electron beam.

The distinction between the radiation pattern produced from a dipole and that from a multipole wiggler is shown clearly in fig. 4. Assuming the magnetic field distribution to be sinusoidal along the direction of electron motion with a peak field amplitude B_0 (T) and a spatial field period (of λ_0 cm) it can be shown that the angular deflection of the electron beam, θ_w (mrads), is given by

$$\theta_w \sim 0.05 B_0 \lambda_0 / E, \quad (10)$$

and the lateral displacement of the beam (mm),

$$a_w \sim 10^{-3} \theta_w \lambda_0 / \pi. \quad (11)$$

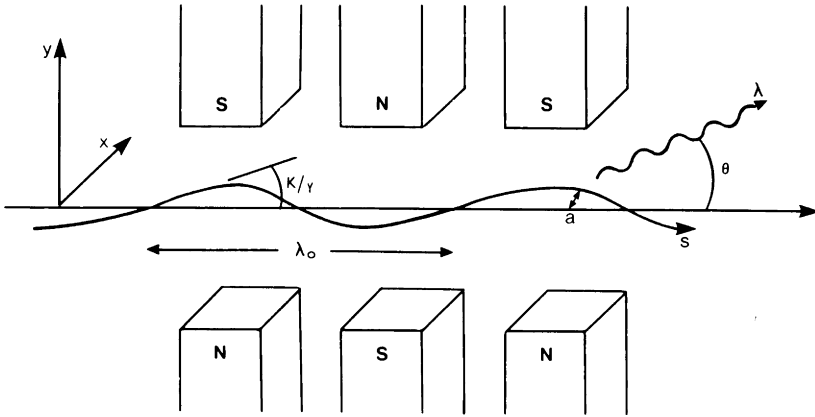


Fig. 4. Radiation pattern from a dipole and a multipole wiggler.

The important parameter, K , is called the deflection parameter, and

$$K \sim 93 B_0 \lambda_0 \quad (12)$$

giving a horizontal angular deflection of $\sim K/\gamma$.

The value of K for wigglers is normally rather large – for example, $K \sim 230$ for the three pole 5 T wiggler on the SRS at Daresbury. The maximum deflection of the electron beam is $\theta_w \sim 60$ mrad, although the radiation divergence in the vertical direction remains $\sim 1/\gamma$, as for conventional synchrotron radiation. The deflection of the electron beam through the SRS wiggler ($a_w = 9$ mm) is also relatively large. Wiggler magnets are generally used as wavelength shifters, that is, to reduce the effective λ_c of the storage ring at the wiggler magnet without recourse to the much more expensive solution which would be to increase the energy E (GeV) of the electron beam. The multipole wigglers therefore simply produce from N poles, N times the intensity from a dipole magnet radiating into about the same solid angle.

In practice, the opening angle for the emitted radiation θ_{ph} will contain a contribution both from the electron beam divergence and from the synchrotron radiation divergence:

$$\theta_{ph}^2 = \theta_w^2 + \left(\frac{1}{\gamma}\right)^2, \quad (13)$$

which can be rearranged to give

$$\theta_w \sim \frac{1}{\gamma} \left(1 + \frac{1}{2} K^2\right). \quad (14)$$

Clearly, when K is large ($\gg 1$) the photon emission angle is dominated by the electron trajectory. However, as K is reduced, for example by reducing the field

strength B_0 or the period (λ_0) of the magnet array, a regime will be reached where all radiation is confined within an angular range $\sim 1/\gamma$ in both vertical and horizontal planes. Devices which operate in this mode are called undulators.

3.2. Undulator radiation

When the insertion device causes the electron beam to perform a series of wiggles by using a large number ($N \sim 100$) equally spaced alternately polarised dipole magnets, it is possible to increase the photon flux seen at the detector by N , the number of single period wiggles. If, however, the spacing λ_0 between the single period wiggles is reduced there comes a time when the radiation is best described by considering the relativistic oscillation of the electron transverse to the motion of the electron beam. In this situation we would expect the electrons to radiate at the oscillation wavelength and the radiation to be more nearly monochromatic. The radiation received at the detector would of course be shifted due to the Doppler effect, so the radiation is shifted from λ_0 to

$$\lambda \sim \frac{\lambda_0}{2\gamma^2}. \quad (15)$$

Taking into account the angular spread of the radiation over an angle θ with respect to the electron beam axis we get for $K < 1$:

$$\lambda = \frac{\lambda_0}{2\gamma^2} (1 + \frac{1}{2}K^2 + \gamma^2\theta^2), \quad (16)$$

so that for $\theta = 0$ a 2 GeV electron traversing a magnetic field configuration with $\lambda_0 = 10$ cm would emit radiation at ~ 3.3 nm, provided K is sufficiently low to be neglected. The power radiated is peaked in the forward direction as is the radiation for the conventional synchrotron source but because of the oscillating motion transverse to the radiation, the radiation pattern is more complex than conventional synchrotron radiation (Hoffman 1980).

As the value of the magnetic field B_0 is increased, the transverse force on the electron increases so that it moves faster and it is then possible to have relativistic transverse motion of the electron superimposed on its relativistic forward motion. Under these conditions any increase in the transverse momentum must be accompanied by a decrease in the longitudinal momentum and vice versa. In the moving frame of reference of the average relativistic drift velocity along the longitudinal axis, the electron executes a figure of eight type of motion instead of the simple harmonic oscillation previously assumed. This motion now contains harmonics of the oscillation frequency, and transformation into the laboratory frame gives a wavelength spectrum,

$$\lambda = \frac{\lambda_0}{2k\gamma^2} (1 + \frac{1}{2}K^2 + \gamma^2\theta^2), \quad (17)$$

where k is the odd harmonic number (1, 3, 5, etc.) which occurs in the forward direction. Increasing K has the effect of smearing out the harmonics and ultimately returning to the continuum of the conventional synchrotron radiation source.

Whether the insertion device is called a multipole wiggler or an undulator depends on the particular configuration of parameters. Wigglers have large K values and essentially are used to increase the power emitted in a particular wavelength region. Undulators have low K values and provide a more peaked selection of quasi-monochromatic radiation. Both devices have their places in the synchrotron radiation source and since, in principle, they can be switched in or out as the experimenters desire, without altering the running of the whole facility, they are economically desirable as well as providing new versatile high flux sources. The total power radiated by an undulator is relatively small ($\sim 20\text{--}30$ W), although for the wavelength of the fundamental the central brightness is extremely high ($\sim 10^4$ that of a bending magnet). Restriction of the central cone of radiation about the electron drift axis by a pinhole could be used to produce essentially monochromatic radiation. In practice, the radiation pattern is also governed by the angular spread of the electron beam so that for example at the SRS, prior to the introduction of the high brightness lattice, there was considerable smoothing out of the spectrum and the undulator served to increase the photon flux over a wide energy band rather than to provide quasi-monochromatic radiation.

3.3. Coherence

Coherence is usually regarded as an exclusive property of the laser. It is of interest in that it refers to the ability to form interference patterns when wave fronts are recombined from a given source. In fact, sources which exhibit partial coherence can be used to produce clear interference fringes provided the displacement of the wave front is kept within limits set by the coherence length,

$$l_c = \frac{\lambda^2}{\Delta\lambda}, \quad (18)$$

where λ is the wavelength and $\Delta\lambda$ the spectral line width of the radiation.

For radiation at 10 nm a value of l_c which is 1–10 μm would be quite useable for many purposes so that the use of undulators as partially coherent sources is now feasible with modern low emittance storage rings. For wave front separations of less than l_c it is possible to observe clear interference patterns and with some improvement in current conditions, soft X-ray interferometry and holography should be feasible.

The radiation from an undulator discussed in section 3.2 would be expected to appear as a group of harmonic lines each of spectral purity: $\lambda/\Delta\lambda \sim kN$. Consequently, the longitudinal coherence length is given by

$$l_c = \frac{\lambda^2}{\Delta\lambda} \sim kN\lambda, \quad (19)$$

which is essentially the relativistically contracted length of the undulator. For $\lambda = 3.3$ nm, $N = 100$ and $k = 3$, $l_c = 1$ μ m. Additionally, by using a monochromator following the undulator, $\lambda/\Delta\lambda$ could be increased by another order of magnitude, with the penalty of course that the power available would be reduced. With coherence lengths of tens of micrometres holographic microscopy with a relatively deep depth of field should be possible.

4. Synchrotron radiation source installations

Around the world, the number of dedicated storage ring sources for synchrotron radiation research is continuing to increase at a rapid rate. This increase is notable in view of the major capital costs associated with the design, construction and operation of any new accelerator (\sim £100 M for high energy 5 GeV storage rings). Although these source costs can present considerable problems to the science community in any country, they are followed in due course by the equally considerable costs associated with the construction and operation of ports, beam lines and experimental stations. Recent years have seen many international collaborative activities in the field of synchrotron radiation research of which the largest and best example is that of the European Synchrotron Radiation Facility (the ESRF) which is approaching an advanced stage in its design at Grenoble in France.

To introduce economies into capital funding, the resources required to develop new beam lines and experimental stations are sometimes provided wholly by the future user of the beam line. This approach has led to the creation of participating research teams or of industrial consortia who are exclusively responsible for an experimental station and actually pay the science community for use of source beam time. The most recent development has been the evolution of specific sources which will be exclusively dedicated to the large scale replication of large area integrated circuit devices with submicron features using soft X-ray radiation. Projects of this kind are at a very advanced stage of development already in the Federal Republic of Germany, the UK, USA and Japan.

Table 1 presents a catalogue of source properties (derived in part from Winick and Watson 1986). The most striking feature of the table is that approximately 700 experimental beam lines and stations will be operating world wide by the beginning of the next decade (1990). This represents a capital investment in experimental equipment alone which will greatly exceed a £1000 M. Collectively, the sources and their associated stations will incorporate several thousands optical elements (mirrors, gratings and crystals) of the very highest optical quality obtainable and this has already led to the creation of a small industry of specialist ultra-high vacuum optical and instrument making companies.

References

- Buras, B., and S. Tazzari, 1985, European Synchrotron Radiation Facility, Rep. ESRP c/o CERN (CERN, Switzerland).
- Hoffman, A., 1980, Phys. Rep. **64**(5), 253.
- Jackson, J.D., 1975, Classical Electrodynamics, 2nd Ed. (Wiley-Interscience, New York) p. 672ff.
- Kincaid, B.M., 1977, J. Appl. Phys. **48**, 2648.
- Koch, E.-E., D.E. Eastman and Y. Farge, 1983, in: Handbook on Synchrotron Radiation, Vol. 1, ed. E.-E. Koch (North-Holland, Amsterdam) ch. 1.
- Krinsky, S., M.L. Perlman and R.E. Watson, 1983, in: Handbook on Synchrotron Radiation, Vol. 1, ed. E.-E. Koch (North-Holland, Amsterdam) ch. 2.
- Lienard, A., 1898, L'Eclairage Electron. **16**, 5.
- Sands, M., 1970, Stanford Linear Accelerator Rep. SLAC (SLA, Stanford, CA) p. 121.
- Schott, G.A., 1912, Electromagnetic Radiation (Cambridge).
- Walker, R.P., 1986, Daresbury Laboratory SCI (Daresbury Laboratory, Daresbury, Warrington) p. 513A.
- Winick, H., and R.E. Watson, 1986, Nucl. Instrum. Methods **222**, 373.

CHAPTER 2

OPTICAL ENGINEERING

J.B. WEST and H.A. PADMORE

*Science and Engineering Research Council, Daresbury Laboratory, Daresbury,
Warrington WA4 4AD, UK*

Contents

1. Introduction	23
2. The synchrotron radiation source	24
2.1. Source emittance	24
2.2. The calculation of synchrotron radiation intensities	28
3. Mirrors	35
3.1. Focusing properties and surface equations of common optical elements	36
3.1.1. The parabola	36
3.1.2. The ellipse	37
3.1.3. Toroids	39
3.2. Reflectivity of mirrors	41
3.3. Separated function mirror systems	52
4. Diffraction grating optics	56
4.1. Application of the grating equation	56
4.1.1. Diffraction	56
4.1.1.1. Spectrograph geometry	57
4.1.1.2. Fixed grating-deviation-angle geometry	57
4.1.1.3. On-blaze geometry	59
4.1.1.4. Plane grating constant-image-distance geometry	61
4.1.1.5. In-focus Miyake geometry	61
4.1.2. Dispersion	62
4.1.3. Entrance and exit slit-width-limited resolution	62
4.2. The geometric aberration theory of diffraction gratings	63
4.2.1. The optical path function	64
4.3. The toroidal grating monochromator.	68
4.4. Design of TGM pre-optics	77
4.5. The astigmatically corrected spherical grating in a TGM mounting; the SGM	78
4.6. Diffraction efficiency	82

Contents continued overleaf

Contents continued

5. Beam line layout	84
5.1. General design principles for a multiple instrument beam line	85
5.2. Details of a four instrument beam line at the Daresbury SRS	88
5.2.1. The normal incidence monochromator (Seya)	88
5.2.2. The high resolution normal incidence monochromator	90
5.2.3. The toroidal grating monochromator	92
5.2.4. The soft X-ray monochromator	93
5.3. Post-focusing optics	97
5.3.1. Remote exit slit	98
5.2.2. Capillary light guide	98
5.3.3. Post-focusing mirrors.	98
6. Optical components	99
6.1. The mounting and adjustment of optical components	100
6.2. Mirror materials	105
6.3. Optical coatings.	108
7. Beam line auxiliary equipment	109
7.1. Laser alignment system	109
7.2. Vacuum equipment	111
7.3. Pressure measuring and monitoring devices	113
7.4. Beam line controls and safety systems	114
7.4.1. Safety aspects	114
7.4.2. Vacuum protection	115
7.4.3. Radiation damage protection	115
8. Conclusion	116
References	117

1. Introduction

Of the many aspects involved in constructing a synchrotron radiation facility, one which is not widely met in other research areas is the close link between large scale mechanical engineering and precision optics. The only other example which comes readily to mind is the construction of large astronomical telescopes, and these have the advantage in general of being single purpose instruments. In contrast, a synchrotron radiation source will be used for a wide variety of experiments covering research areas in physics, chemistry, biology, and applied areas such as material science and technology. The means of bringing the radiation from the orbiting electrons onto the experimental sample with maximum efficiency is therefore highly important, and the experimental requirements vary considerably in this respect. The “beam line” is the means of bringing the “white” radiation to the monochromator and/or experiment, and in general is far from being just a straight piece of pipe between the experiment and the synchrotron radiation source. It may have to feed three or more experiments covering a wide spectral range from the soft X-ray to the near ultraviolet, in addition to being the interface between the experimental vacuum environment and the ultrahigh vacuum of the source. It must also provide users with protection against damaging radiation, particularly in those cases where the electron beam energy in the source exceeds a few hundred MeV. Thus a beam line is often a very complex assembly; due allowance should always be made for the fact that the capital cost in providing a complete set of beam lines on an electron storage ring designed for synchrotron radiation work will far exceed the capital cost of the accelerator itself.

It is the purpose of this chapter to identify the main problems in constructing beam lines for synchrotron radiation and to show how precision optics can be integrated into the general beam line design; hence the term “optical engineering”. It is not our intention to review all the beam lines and monochromators on facilities throughout the world, since the literature already contains a wealth of such information. We set out to identify fundamental concepts and good design practice, and hope that these, together with examples of beam line designs presently used, will be helpful to those in the process of designing beam lines for future synchrotron radiation sources.

In many respects, the monochromatising element is an integral part of beam line optical design and the two should be considered as one system. As can be seen from the chapter on VUV (vacuum ultraviolet) monochromators in Volume 1 of this Handbook (R.L. Johnson 1983) there are many designs presently available, and, contrary to the situation a few years ago, any experimental requirement can probably be met by one of these designs. Some of these instruments have been well characterised (see a summary by Ederer 1982, also Saile and West 1983) and a few are available commercially as complete working

monochromators. The view taken here is that, as a starting point the monochromators required for the experimental programme in mind should be designed first and the beam line, with all the preoptics involved, designed to incorporate them. As will be seen later, when fitting three or four monochromators into a beam line compromises are inevitable and restraints on the optical design can arise when considering the construction of the whole assembly. There are also applications, (e.g. extremely high aperture, or very large resolving power) where one instrument will dominate beam line design. We shall be concerned primarily with beam lines on which more than one experimental facility is located, although design details for single experiment lines will be considered.

Another factor which enters into beam line design is the wavelength range to be covered, in particular whether experiments using wavelengths shorter than 4 Å, the longest practical wavelength at which a beryllium window can be used, are to be mixed with longer wavelength experiments on the same beam line. For low-energy synchrotron radiation sources this does not apply, but on higher energy or “compromise” sources there are good practical reasons to separate beam lines which have beryllium windows and whose experiments run in air or helium atmospheres from those which run in vacuum. One primary reason is the need for shielded hutches around experiments where there are X-ray paths in air; it is a considerable simplification not to mix shielded experiments with unshielded ones. In addition, so-called X-ray beam lines are simpler in construction and less demanding from the vacuum point of view. This chapter will concentrate on design principles and practical considerations for VUV/soft X-ray beam lines.

Thus we begin with a description of basic source requirements, followed by methods of calculating the light flux from the source. Focusing properties of optical elements and aberration theory will then be considered, since a knowledge of these is essential before a final beam line design, in which the instruments are integrated with the source, can be reached. For general information purposes, a section on the behaviour and choice of optical coatings is included, since, although this has no direct effect on beam line layout, it has a marked effect on beam line performance.

2. The synchrotron radiation source

2.1. Source emittance

There can be little doubt that a prime requirement of a VUV source is small emittance, where emittance is defined by considering the behaviour of the electron beam in phase space. If we define the direction along which the electrons move as the s direction, x and y perpendicular to this direction in and perpendicular to the orbit plane, respectively, then phase space coordinates are x and x' , y and y' , where $x' = dx/ds$ and $y' = dy/ds$.

Thus x' is the angle the electrons make with the straight ahead direction in the orbit plane, and y' , correspondingly, perpendicular to the orbit plane. In general

these angles are small enough that the approximation $\tan^{-1} dx/ds = dx/ds$, $\tan^{-1} dy/ds = dy/ds$ can be made. Figure 2.1 shows examples of electron beam cross sections in configuration and phase space, and fig. 2.2 shows the phase space ellipses at $s = 0$ chosen to be at a waist of the electron beam cross section, and at a point distance s along the orbit from it, referring to the y direction. The ellipses in figure 2.2 are “one σ ” contours, and thus the “one σ ” emittance is $\sigma_y \sigma_{y'}$, the equation of the ellipse being

$$\frac{\sigma_{y'}}{\sigma_y} y^2 + \frac{\sigma_y}{\sigma_{y'}} y'^2 = \sigma_y \sigma_{y'}$$

Similar relations hold for the x direction.

Thus the emittances in the x and y directions are a combination of the electron beam dimension and the angular divergence of the electrons, both of which vary with position along the direction of travel, s . In reality one observes a finite length of arc of the electron trajectory rather than a single point on the trajectory. It is

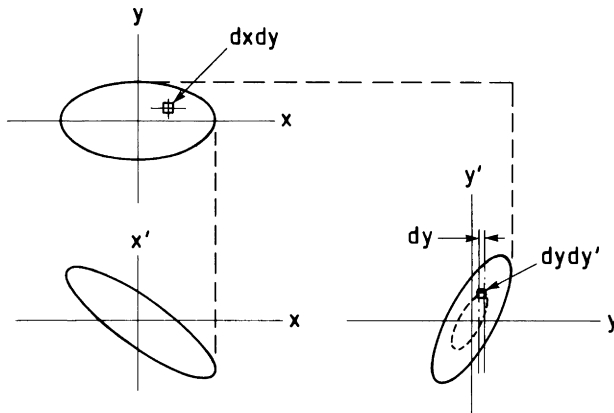


Fig. 2.1. Electron beam cross sections in phase space.

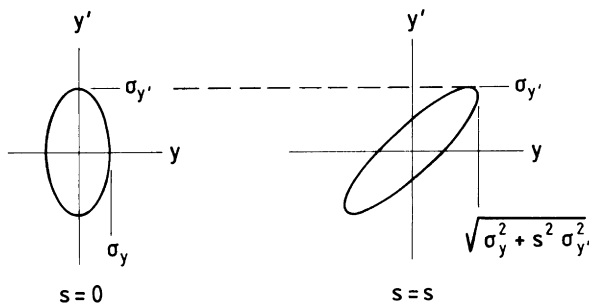


Fig. 2.2. Phase space ellipse at $s = 0$ (waist).

then reasonable to select a midpoint on the arc and project the radiation from points either side of this onto a plane perpendicular to the electron trajectory at this midpoint, the midpoint lying in this plane. This is shown diagrammatically in fig. 2.3 for the yy' phase space. The midpoint ($s=0$) is chosen to be at an electron beam waist. Hence the phase ellipse (1) is vertical. Moving to s , and assuming no magnetic focusing, the ellipse transforms to a slanted ellipse (2) where $\sigma_{y'}$ remains constant but σ_y increases. The divergence angle of the radiation emitted, an angle which varies with optical wavelength, then increases $\sigma_{y'}$, to give the real source at $s = s$ (3). This is then transformed back onto $s = 0$ (4), where the angles are preserved, but the source has increased in apparent size. $\sigma_{y'}$ has become $(\sigma_{y'}^2 + \sigma^2)^{1/2}$, where σ refers to the *photon* angular distribution.

Full mathematical details of all these transformations, and calculations of photon flux from a real source, are to be found in two comprehensive documents by Green (1976, 1977). Clearly, the equations have to be integrated over the full source length (i.e. from $s = -s$ to $s = +s$) in order to map all points of the orbit seen by the beam line optical system onto the plane at $s = 0$. The reader is therefore referred to Green's papers for full mathematical details; his notation has been used here. It is sufficient for present purposes, having presented the basic ideas of the beam optics, to consider which are the dominant source parameters. Good source design should ensure minimum emittance, and provide beam line access to those points in the storage ring lattice where this is a minimum. A factor which influences the vertical beam size is the coupling between horizontal and vertical oscillations of the electron beam; when kept to a minimum this gives the characteristic letter box shape of the electron beam, and thus matches vertically dispersing instruments well. The coupling between the horizontal and vertical oscillations can be kept down to the 1% level with proper design and precise installation of the magnetic components; fig. 2.4 shows the standard deviations for

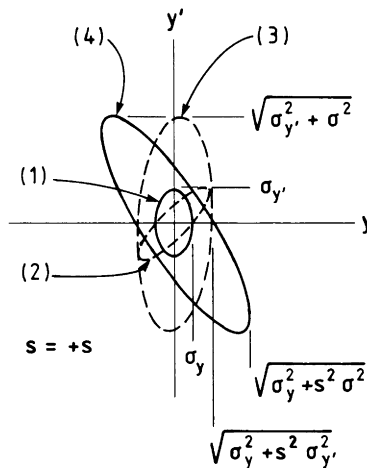


Fig. 2.3. Projection onto a plane at the extended source midpoint.

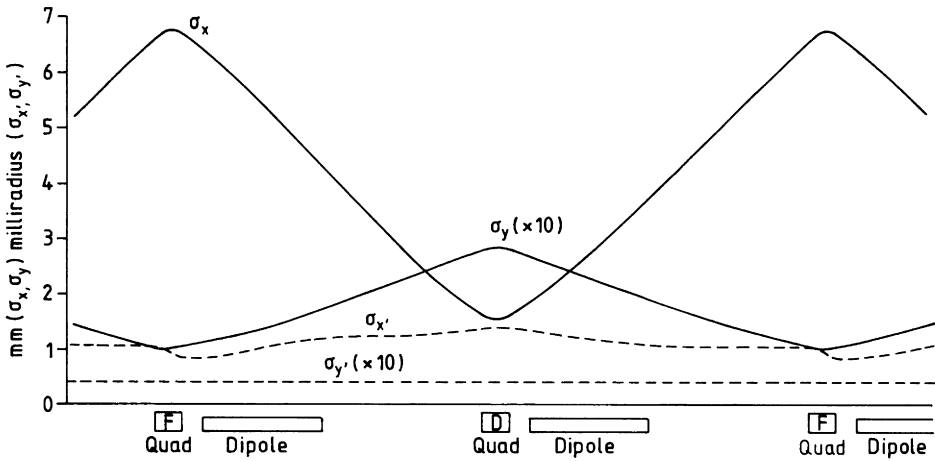


Fig. 2.4. Source size and emittance in the Daresbury SRS.

the source size and emittance for the present magnet lattice in the Daresbury synchrotron radiation source. In fact this is not a low emittance source compared to the VUV rings at Brookhaven and Berlin, where the emittances are at least a factor of 10 smaller, but the point to realise here is that the major contribution to the emittance figure comes from the physical source size; the contribution from the different angular trajectories is substantially less than the divergence of the emitted radiation as far as the VUV and soft X-ray region is concerned. Figure 2.5 shows the improved emittance expected from the modified SRS (Walker

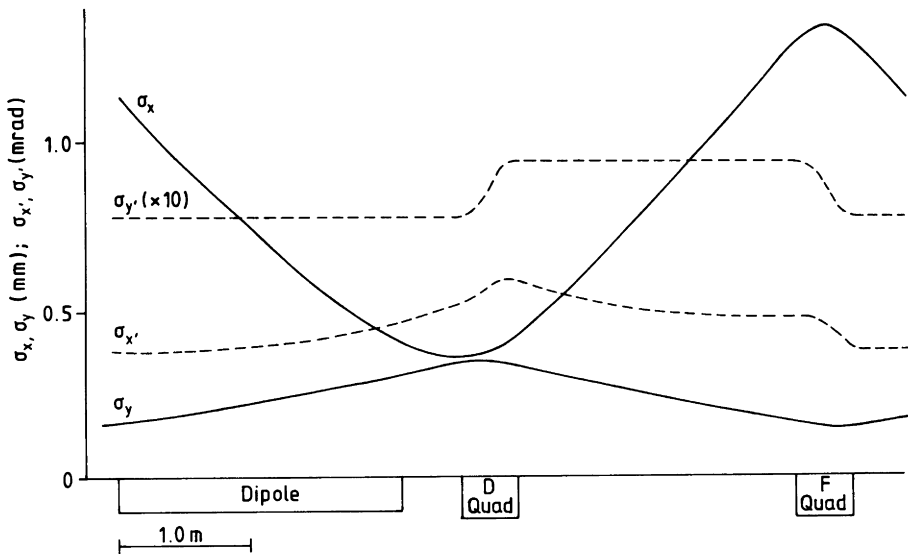


Fig. 2.5. As fig. 2.4, but after the high-brightness lattice modification.

1985). Thus in calculating the apertures (and thus sizes) of collimating or focusing mirrors to collect radiation from the source and feed it to monochromators, the main parameters to consider are source size and the vertical angular divergence resulting from the properties of the radiation itself. The former is provided by the source designer; the latter can be found in published calculations, though not always in a useful form. Thus the next section is devoted to deriving the most useful equations for calculation of the synchrotron radiation flux.

2.2. The calculation of synchrotron radiation intensities

The basic equations describing synchrotron radiation have been given by Schwinger (1949), Sokolov and Ternov (1968), and Tomboulian and Hartman (1956), the latter giving a quantitative comparison between measured synchrotron radiation spectra and the basic theory. Several review papers have been published detailing the properties of synchrotron radiation and their numerical evaluation, of which those by Mack (1966) and by Green (1976, 1977) are the most useful. Several other more general papers have been given by Winick (1980), Codling (1973) and Rowe (1973). The most useful forms of the equations given in the above references are considered here.

The number of photons per second radiated from a tangent point can be expressed in several forms, the most useful being the following.

$$N_k(\lambda) = 1.256 \times 10^{10} k \gamma y G_0(y) \text{ photons}/k\lambda, \text{ s, mA, mrad } \theta. \quad (2.1)$$

Equation (2.1) gives the number of photons per unit bandwidth k .

$$N_{\Delta\lambda}(\lambda) = 0.2998 \frac{\gamma^4}{\rho} y^2 G_0(y) \text{ photons}/\text{\AA}, \text{ s, mA, mrad } \theta. \quad (2.2)$$

Equation (2.2) gives the number of photons per angstrom.

$$N_{\Delta E}(\lambda) = 1.013 \times 10^6 \gamma \lambda_c G_0(y) \text{ photons/eV}, \text{ s, mA, mrad } \theta. \quad (2.3)$$

Equation (2.3) gives the number of photons per electron volt photon energy.

$$P(\lambda) = 1.421 \times 10^{-26} \frac{\gamma^7}{\rho^2} y^3 G_0(y) \text{ W}/\text{\AA}, \text{ mA, mrad } \theta. \quad (2.4)$$

Equation (2.4) gives the power radiated per angstrom. These four equations apply to the case where the radiation spectrum is integrated over all vertical angles φ . The terms used in eqs. (2.1)–(2.5) are as follows:

- ρ : bending magnet radius (m),
- θ : horizontal opening angle (mrad),
- V : machine energy (GeV),

φ : vertical angle from the storage ring plane (mrad),

λ : wavelength (\AA),

γ : 1957 V (GeV),

λ_c : critical wavelength; equal power is radiated above and below the critical wavelength. $\lambda_c = 5.59\rho/V^3$ (\AA),

$y = \lambda_c/\lambda = E_c/E$.

Function G_0 is defined as

$$G_0(y) = \int_y^{\infty} K_{5/3}(x) dx, \quad (2.5)$$

where $K_{5/3}(x)$ is a modified Bessel function of the second kind. Bessel functions of this type can be related to normal modified Bessel functions of non-integral order by the following relation:

$$K_\nu(x) = \frac{\pi}{2} \frac{[I_{-\nu}(x) - I_\nu(x)]}{\sin \nu\pi}. \quad (2.6)$$

For small arguments (e.g. $\nu = 5/3$ and $1/3 < x < 3.0$) $I_\nu(x)$ can be evaluated using a series approximation,

$$I_\nu(x) = \sum_{s=0}^{\infty} \frac{1}{s!(s+\nu)!} \left(\frac{x}{2}\right)^{2s+\nu},$$

$$I_{-\nu}(x) = \sum_{s=0}^{\infty} \frac{1}{s!(s-\nu)!} \left(\frac{x}{2}\right)^{2s-\nu}. \quad (2.7)$$

The non-integer factorials can be evaluated for large arguments using Stirling's approximation and extended to lower values using the factorial difference relation

$$s! = \sqrt{2\pi} s^{s+1/2} e^{-s} (1 + 1/12s) \quad \text{Stirling's approximation}, \quad (2.8)$$

$$(s-1)! = \frac{s!}{s} \quad \text{difference relation}. \quad (2.9)$$

An alternative method is to calculate $s!$ in the range $0 \leq s \leq 1$ from a fitted polynomial and extend to higher values using the difference relation

$$s! = 1 + \sum_{n=1}^8 b_n s^n. \quad (2.10)$$

A polynomial fit of this type has been made by Hastings (1955) with an error of less than 3×10^{-7} . Negative factorials can be found using the relation

$$-s! = \frac{1}{s!} \left(\frac{\pi s}{\sin \pi s} \right). \quad (2.11)$$

For arguments of $K_\nu > 3$, an asymptotic approximation can be used:

$$K_\nu(x) = \left(\frac{\pi}{2x}\right)^{1/2} e^{-x} \left[1 + \frac{(4\nu^2 - 1)}{8x} + \frac{(4\nu^2 - 1)(4\nu^2 - 9)}{2!(8x)^2} + \dots \right]. \quad (2.12)$$

The series form for $x \leq 3$ and the asymptotic form for $x \geq 3$ has been used by Poole (1975, 1976a, b) for the calculation of synchrotron radiation spectra. A more convenient form of $K_\nu(x)$ is given by Arfken (1970) and by Abramowitz and Stegun (1972):

$$K_\nu(x) = \int_0^\infty e^{-x \cosh t} \cdot \cosh \nu t \, dt. \quad (2.13)$$

The form has been directly evaluated using a numerical integration technique by Williams and Weisenbloom (1979). A rapidly converging series form of $K_\nu(x)$ which can be computed faster than the previously given forms has been given by Kostroun (1980):

$$K_\nu(x) = h \left[\frac{1}{2} e^{-x} + \sum_{r=1}^\infty e^{-x \cosh(rh)} \cdot \cosh(\nu rh) \right], \quad (2.14)$$

where h is a small interval. For the computation of G_0 (eq. 5) required in the calculation of synchrotron radiation spectra we require the integral of $K_\nu(x)$ from λ_c/λ to infinity. This can be obtained by numerical integration of $K_\nu(x)$, or using an expression related to eq. (2.14) given by Kostroun (1980):

$$\int_y^\infty K_\nu(x) = h \left[\frac{1}{2} e^{-x} + \sum_{r=1}^\infty e^{-x \cosh(rh)} \frac{\cosh(\nu rh)}{\cosh(rh)} \right]. \quad (2.15)$$

For $\nu = 1/3$ or $2/3$ the series can be truncated at $r = 20$. The expressions given in eqs. (2.1)–(2.4) give the vertically integrated photon flux and radiated power. As many beam line optical systems cannot vertically integrate and in some cases have a variable aperture (e.g. a grating of fixed length scanning in wavelength), it is important to know the variation of flux with vertical angle φ . For a given wavelength, the variation of parallel and perpendicular components of the electric vector (with respect to the storage ring plane) can be given by

$$F_{\parallel}(\varphi) = [1 + (\gamma\varphi)^2]^2 K_{2/3}^2 \left\{ \frac{\lambda_c}{2\lambda} [1 + (\gamma\varphi)^2]^{3/2} \right\}, \quad (2.16)$$

$$F_{\perp}(\varphi) = (\gamma\varphi)^2 [1 + (\gamma\varphi)^2] K_{1/3}^2 \left\{ \frac{\lambda_c}{2\lambda} [1 + (\gamma\varphi)^2]^{3/2} \right\}. \quad (2.17)$$

The degree of linear polarisation can then be found directly from